Supplimentary Information

# Quest for an intermolecular Au(III)···Au(III) interaction between cyclometalated gold(III) cations

**Wei Lu,[a,b] Kaai Tung Chan,[a] Shui-Xing Wu,[a] Yong Chen,[a] and Chi-Ming Che*[a]**

[a] *Department of Chemistry, Institute of Molecular Functional Materials, and HKU-CAS Joint Laboratory on New Materials, The University of Hong Kong, Pokfulam Road, Hong Kong SAR, P. R. China. E-mail: cmche@hku.hk*

[b] *Division of Science, South University of Science and Technology of China, 1088 Xueyuan Boulevard, Shenzhen, Guangdong 518055, P. R. China*

## Experimental Section and Calculation Details

**Experimental Section**

All starting materials were purchased from commercial sources and used as received. The solvents used for synthesis were of analytical grade unless stated otherwise. The solvents used for nanostructure preparations and photophysical measurements were of HPLC grade.

Fast atom bombardment (FAB) mass spectra were obtained on a Finnigan MAT 95 mass spectrometer using 3-nitrobenzyl alcohol as matrix. $^{1}$H NMR spectra were recorded on a Bruker Avance 400 FT-NMR spectrometers. UV-vis absorption spectra were recorded on a Perkin-Elmer Lambda 19 UV/vis spectrophotometer. Steady-state emission spectra were obtained on a SPEX 1681 Fluorolog-2 series F111AI fluorescence spectrophotometer. TEM and SAED were performed on a Philips Tecnai G2 20 S-TWIN transmission electron microscope with an accelerating voltage of 200 kV. The TEM images and SAED patterns were taken by Gatan MultiScan Camera Model 794. TEM samples were prepared by depositing a few drops of suspensions on the formvar-coated copper grids and the excess solvent was removed by a piece of filter paper. The SEM images were taken on a Hitachi S-4800 field emission scanning electron microscope operating at 3.0 kV. SEM samples were prepared by drop-casting suspensions onto silicon wafers. No gold or platinum sputtering was applied before SEM observations.

Crystals of **5** suitable for single crystal X-ray diffraction experiment were obtained by slow diffusion of diethyl ether vapour into acetonitrile solution. Crystals of **5** lose solvated solvent molecules in air at room temperature and collapse easily. Thus a needle-like single crystal was carefully sealed into a capillary and subjected for diffraction study. The diffraction data were collected at 100 K on a Bruker X8 PROTEUM

single crystal X-ray diffractometer with MicroStar rotating-anode X-ray source ($CuK_\alpha$ radiation, $\lambda = 1.54178$ Å).

**Synthesis and Characterization**

**[Au(C^N^N)OAc](PF$_6$):** Gold(III) acetate (107 mg, 0.286 mmol) and 6'-phenyl-2,2'-bipyridine (65 mg, 0.28 mmol) were added to acetic acid (10 mL). The mixture was heated at 80$^o$C for 24 hours. The yellow solution was cooled down to room temperature and filtered. The volume of the filtrate was reduced to around 1 mL under vacuum. Methanol (3 mL) was added and the resultant solution was filtered into a saturated methanolic solution of ammonium hexafluorophosphate. Yellow precipitates were collected, washed with water, a little methanol and diethyl ether. Yield: 157 mg, 88.7%. MS FAB: *m/z* 428 [$M^+$]; $^1$H NMR (400 MHz, $CD_3CN$): $\delta$ 5.30 (s, 3H, $CH_3COO$), 7.26 (d, 1H), 7.50 (t, 1H), 7.58 (t, 1H), 7.83 (dd, 1H, $J$ = 2.1 Hz), 8.06 (dt, 1H), 8.15 (d, 1H), 8.25 (d, 1H), 8.47 (d, 1H), 8.52−8.53 (t, 2H), 8.85 (d, 1H). Elemental analyses Calcd for $C_{18}H_{24}AuF_6N_2O_2P$: C, 34.19; H, 2.23; N, 4.43. Found: C, 33.70; H, 2.35; N, 4.38.

**General Procedure for the Syntheses of Complexes 1–5:** A mixture of arylacetylene (0.095 mmol) and potassium hydroxide (12 mg, 0.30 mmol) in methanol was stirred for two hours at room temperature. [Au(C^N^N)OAc](PF$_6$) (40 mg, 0.063 mmol) was added to the reaction mixture and stirred further for 2 hours. After filtration, the resulted yellow or violet solid was filtered out and washed thoroughly with water, methanol and diethyl ether to afford pure product in good yields.

**[Au(C^N^N)(C≡CC$_6$H$_5$)](PF$_6$) (1)**: Yield: 20 mg, 46.9%. MS FAB: *m/z* 529 [$M^+$]; $^1$H NMR (400 MHz, $CD_3CN$) $\delta$ 7.43−7.47 (m, 3H), 7.52 (t, 1H), 7.62−7.64 (m, 2H),

7..85−7.87 (dd, 1H), 8.05 (dd, 1H), 8.09 (dt, 1H), 8.45 (d, 1H), 8.55−8.62 (m, 3H), 8.83 (d, 1H), 9.07 (d, 1H).

**[Au(C^N^N)(C≡CC$_6$H$_4$-4-CH$_3$)](PF$_6$) (2)**: Yield: 26 mg, 59.7%. MS FAB: *m/z* 543.1 [M$^+$]; $^1$H NMR (400 MHz, CD$_3$CN) $\delta$ 7.07 (t, 1H), 7.11−7.13 (d, 2H), 7.17−7.19 (d, 2H), 7.27 (t, 1H), 7.39 (dd, 1H), 7.54 (dd, 1H), 7.72 (dt, 1H), 7.83−7.85 (d, 1H), 8.00 (d, 1H), 8.17−8.27 (m, 3H), 8.75 (d, 1H).

**[Au(C^N^N](C≡CC$_6$H$_4$-4-C$_6$H$_5$)](PF$_6$) (3)**: Yield: 13.9 mg, 29.3%. MS FAB: *m/z* 605.1 [M$^+$]; $^1$H NMR (400 MHz, CD$_3$CN) $\delta$ 7.40−7.43 (m, 2H), 7.43−7.53 (m, 3H), 7.67−7.72 (m, 6H), 7.81 (dd, 1H), 7.92 (d, 1H), 7.98 (dt, 1H), 8.12 (d, 1H), 8.23 (d, 1H), 8.39 (t, 1H), 8.44−8.46 (m, 2H), 9.10 (d, 1H).

**[Au(C^N^N](C≡CC$_6$H$_4$-4-OCH$_3$)](PF$_6$) (4)**: Yield: 12 mg, 26.9%. MS FAB: *m/z* 559.0 [M$^+$]; $^1$H NMR (400 MHz, CD$_3$CN) $\delta$ 3.85 (s, 3H, OCH$_3$), 6.93−6.96 (d, 2H), 7.33 (t, 1H ), 7.44 (d, 1H), 7.47−7.49 (d, 2H), 7.75 (d, 1H), 7.79 (d, 1H), 7.92 (dt, 1H), 8.06 (d, 1H), 8.18 (d, 1H), 8.35 (t, 1H), 8.40−8.41 (d, 2H), 9.01 (d, 1H).

**[Au(C^N^N)(C≡CC$_6$H$_4$-4-NMe$_2$)](PF$_6$) (5):** Yield: 30.3 mg, 66.8%. MS FAB: *m/z* 572.1 [M$^+$]; $^1$H NMR (400 MHz, CD$_3$CN) $\delta$ 2.99−3.00 (s, 6H), 6.66−6.69 (dd, 2H), 7.29−7.33 (m, 3H), 7.43 (dt, 1H), 7.73−7.77 (t, 2H), 7.90 (m, 1H), 8.03 (d, 1H), 8.14 (d, 1H), 8.33 (t, 1H), 8.38−8.39 (dd, 2H), 8.99 (d, 1H). Elemental analyses Calcd for C$_{26}$H$_{21}$AuF$_6$N$_3$P: C, 43.53; H, 2.95; N, 5.86. Found: C, 43.70; H, 3.22; N, 5.88.

**Table S1.** Crystal Data

| | |
|---|---|
| Empirical formula | $C_{28}H_{21}F_6N_4PAu$ |
| Formula weight | 755.42 |
| Temperature | 100(2) K |
| Wavelength | 1.54178 Å |
| Crystal system | Monoclinic |
| Space group | $P\,2_1/c$ |
| Unit cell dimensions | $a$ = 16.2749(9) Å .<br>$b$ = 7.2655(4) Å<br>$c$ = 22.8836(13) Å<br>$\beta$= 91.975(2)° |
| Volume | 2704.3(3) $Å^3$ |
| $Z$ | 4 |
| Density (calculated) | 1.855 $mg/m^3$ |
| Absorption coefficient | 11.388 $mm^{-1}$ |
| $F(000)$ | 1460 |
| $\theta$ range for data collection | 2.72 to 65.25°. |
| Index ranges | -19<=h<=17, -6<=k<=8, -26<=l<=26 |
| Reflections collected | 17107 |
| Independent reflections | 4311 [$R_{int}$ = 0.0425] |
| Completeness to theta = 25.63° | 93.5 % |
| Absorption correction | None |
| Refinement method | Full-matrix least-squares on $F^2$ |
| Data / restraints / parameters | 4328 / 0 / 363 |
| Goodness-of-fit on $F^2$ | 1.070 |
| Final $R$ indices [$I > 2\sigma(I)$] | $R_1$ = 0.0607, $wR_2$ = 0.1531 |
| $R$ indices (all data) | $R_1$ = 0.0713, $wR_2$ = 0.1623 |
| Largest diff. peak and hole | 3.312 and -1.380 $eÅ^{-3}$ |

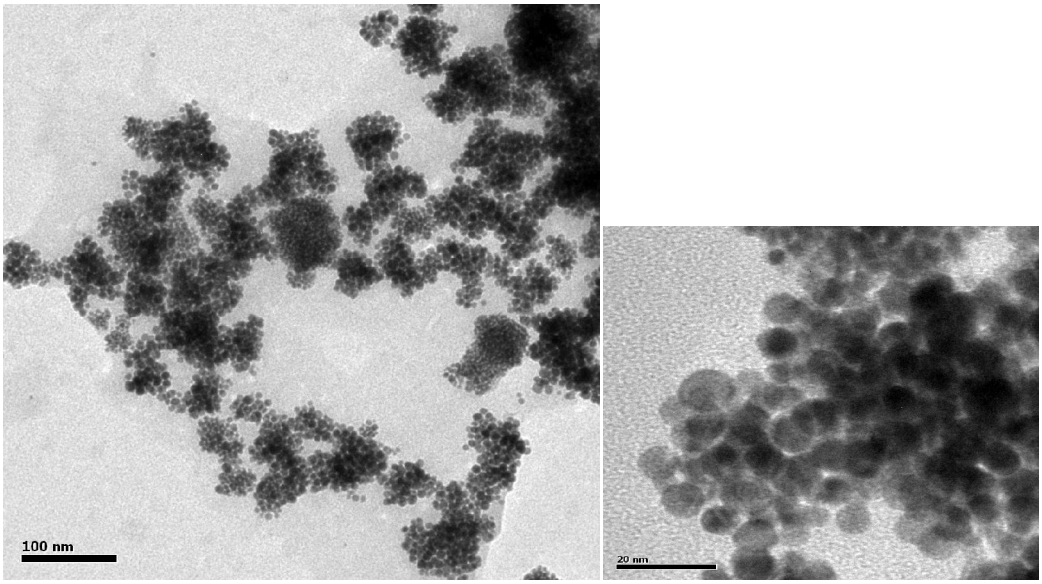


**Figure S1.** TEM of [Au(C^N^N)(C≡C$C_6H_4$-4-OMe)]($PF_6$) (**4**) after standing in MeCN for 7 days.

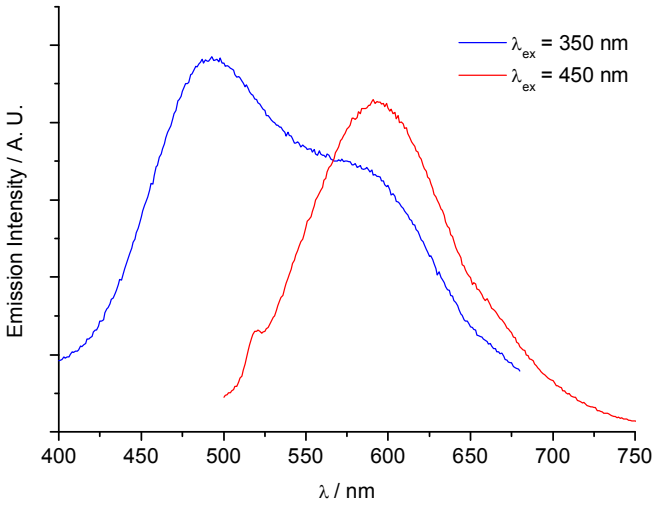


**Figure S2.** Emission spectra of complex **5** in DMF solution at various excitation wavelengths. Concentration ~$2.0\times10^{-5}$ M.

**Calculation Details**

These analyses on the weak bonding interactions were based the crystal structure without geometry optimization. Considering noncovalent interactions, the long-range dispersion-corrected functional SSB-D was employed. The energy decomposition analysis (EDA) on the Au(III)…Au(III) paired cations of **5** was conducted using TZ2P basis set, with cooperation of zero-order zero order regular approximation (ZORA) for the relativistic effects. EDA and ETS-NOCV calculations were finished by ADF program.[1, 2]

The optimizations, potential energy curve scans, and excited state calculations were performed using PBE0 implemented in program Gaussian 09.[3] Ahlrich's def2-TZVP[4] basis set was used and salvation effects of the acetonitrile solvent were modeled by the polarizable continuum model (PCM)[5]. For the consitance with electronic spectra analyses, in which a suitable hybrid functional is necessary for accurately characterizing the electronic transition involving change transfer characters, PBE0 was used for single-point calculations on the crystal structures to analysis the orbitals of the dimer.

[1] *ADF2010*, SCM, Theoretical Chemistry, Vrije Universiteit, Amsterdam, The Netherlands, http://www.scm.com.

[2] G. T. Velde, F. M. Bickelhaupt, E. J. Baerends, C. F. Guerra, S. J. A. Van Gisbergen, J. G. Snijders and T. Ziegler, *J. Comput. Chem.* **2001**, *22*, 931-967.

[3] M. J. Frisch, G. W. Trucks, H. B. Schlegel, G. E. Scuseria, M. A. Robb, J. R. Cheeseman, G. Scalmani, V. Barone, B. Mennucci, G. A. Petersson, H. Nakatsuji, M. Caricato, X. Li, H. P. Hratchian, A. F. Izmaylov, J. Bloino, G. Zheng, J. L. Sonnenberg, M. Hada, M. Ehara, K. Toyota, R. Fukuda, J. Hasegawa, M. Ishida, T. Nakajima, Y. Honda, O. Kitao, H. Nakai, T. Vreven, J. A. Montgomery, Jr., J. E. Peralta, F. Ogliaro, M. Bearpark, J. J. Heyd, E. Brothers, K. N. Kudin, V. N. Staroverov, R. Kobayashi, J. Normand, K. Raghavachari, A. Rendell, J. C. Burant, S. S. Iyengar, J. Tomasi, M. Cossi, N. Rega, J. M. Millam, M. Klene, J. E. Knox, J. B. Cross, V. Bakken, C. Adamo, J. Jaramillo, R. Gomperts, R. E. Stratmann, O. Yazyev, A. J. Austin, R. Cammi, C. Pomelli, J. W. Ochterski, R. L. Martin, K. Morokuma, V. G. Zakrzewski, G. A. Voth, P. Salvador, J.

J. Dannenberg, S. Dapprich, A. D. Daniels, O. Farkas, J. B. Foresman, J. V. Ortiz, J. Cioslowski and D. J. Fox, Gaussian 09, Revision A.02; Gaussian, Inc., Wallingford CT, 2009.

[4] F. Weigend and R. Ahlrichs, *Phys. Chem. Chem. Phys.* **2005**, *7*, 3297-3305.

[5] M. Cossi, V. Barone, B. Mennucci and J. Tomasi, *Chem. Phys. Lett.* **1998**, *286*, 253-260.

[6] C. Adamo and V. Barone, *The Journal of Chemical Physics* **1999**, *110*, 6158-6170.

**Table S2.** Complex **5**: EDA results and portioned dispersion components calculated by SSB-D/TZ2P.

| Total Term | Energy Decomposed Terms | | | |
|---|---|---|---|---|
| $\Delta E_{int}$ | $\Delta E_{elstat}$ | $\Delta E_{pauli}$ | $\Delta E_{orb}$ | $\Delta E_{disp}$ |
| -4.20 | 21.26 | 29.74 | -16.07 | -39.13 |
| | Partioned Dispersion Components[a] | | | |
| | Ligand~Ligand′ | Au~Au′ | Ligand~Au′ | Ligand′~Au |
| | -24.72 | -3.89 | -5.26 | -5.26 |

[a] the ligand presents one whole cation monomer but the atom Au.

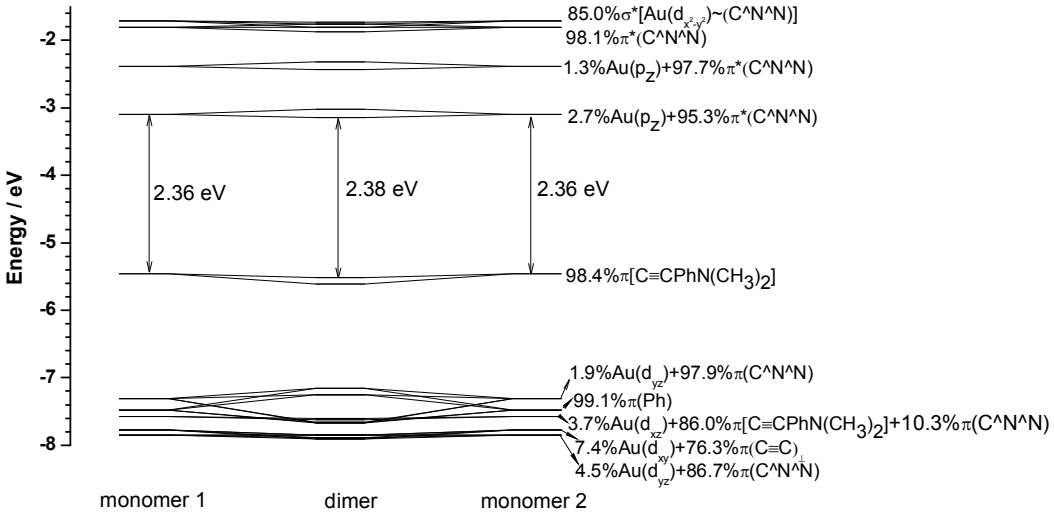


**Figure S3.** Diagram for orbital interactions between two monomers of complex **5** by PBE0/def2-TZVP calculations on the structure from the crystal data with solvation of solvation of acetonitrile.

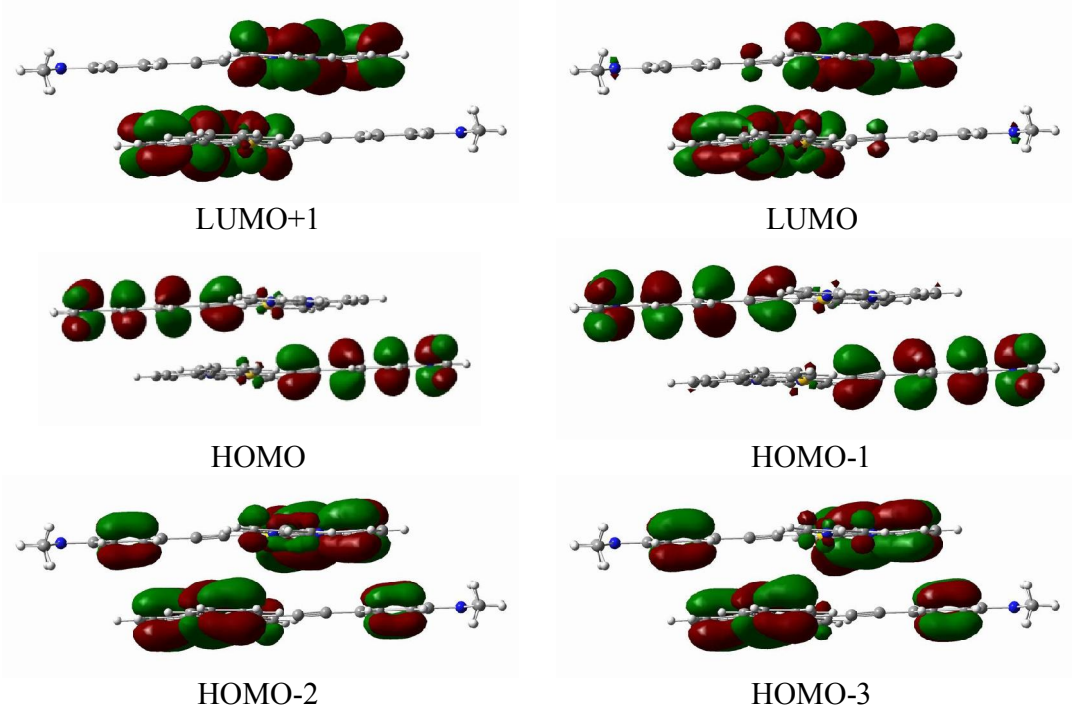


**Figure S4.** Diagram for molecular orbitals calculated on the dimeric structure of complex **5** from the crystal data.

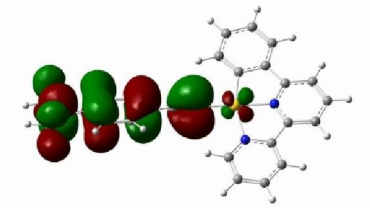

HOMO: 1.3%Au($d_{xz}$)+97.7%$\pi_{[C\equiv CPhN(CH3)2]}$

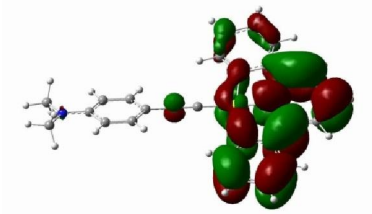

LUMO: 3.1%Au($p_z$)+94.2%$\pi_{(C^N^N)}$

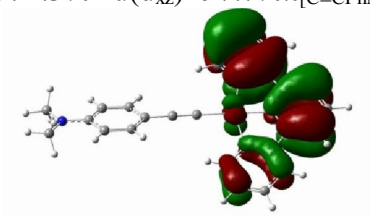

HOMO-1: 3.9%Au($d_{yz}$)+ 97.9%$\pi_{(C^N^N)}$

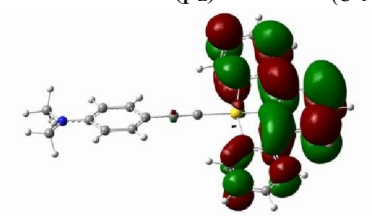

LUMO+1: 1.0%Au($p_z$)+98.2%$\pi_{(C^N^N)}$

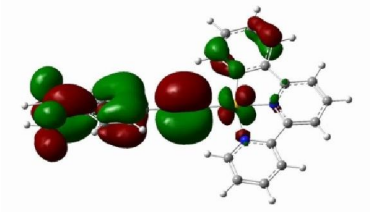

HOMO-2: 3.9%Au($d_{xz}$)+89.5%$\pi_{[C\equiv CPhN(CH3)2]}$+6.7%$\pi_{(C^N^N)}$

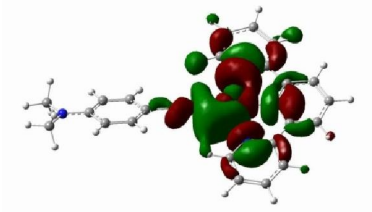

LUMO+2: 84.4%$\sigma^*_{[Au(d_{y2}^{x2-})\sim(C^N^N)]}$

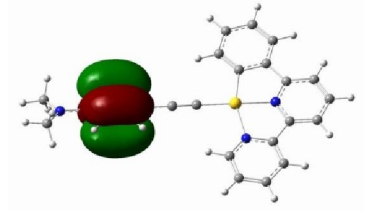

HOMO-3: 99.6%$\pi_{(Ph)}$

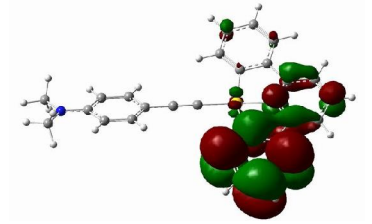

LUMO+3: 99.5%$\pi^*_{(C^N^N)}$

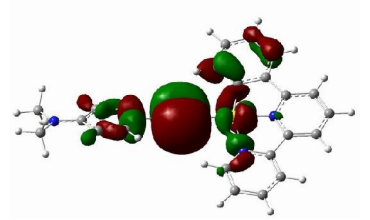

HOMO-4: 7.0%Au($d_{xy}$)+76.9%$\pi_{(C\equiv C)\perp}$

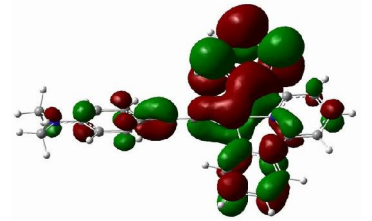

LUMO+4: 5.8%Au($p_z$)+4.8%$\pi^*_{(C\equiv C)}$+82.8%$\pi^*_{(C^N^N)}$

**Figure S5.** Selected frontier molecular orbitals of complex **5** calculated on the PBE0/def2-TZVP optimized geometry.

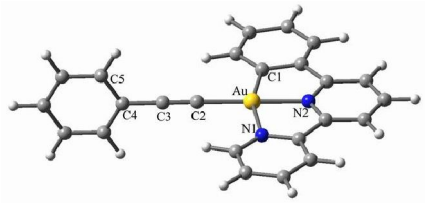


**1** ( $D_{C1\text{-}Au\text{-}C4\text{-}C5}$ = 89.5º )

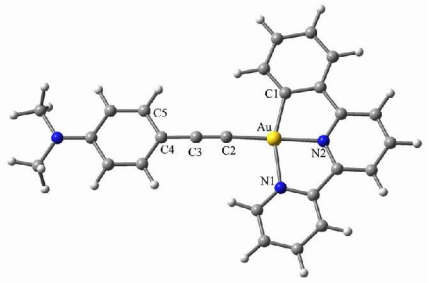


**5** ( $D_{C1\text{-}Au\text{-}C4\text{-}C5}$ = 29.2º )

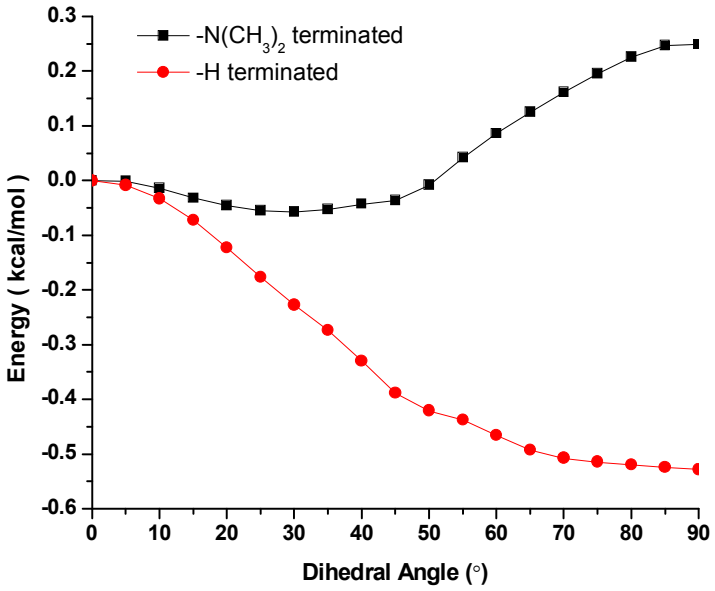


**Figure S6.** PBE0 Optimized structures in Gas Phase ($D_{C1\text{-}Au\text{-}C4\text{-}C5}$ represents the dihedral angle between atoms C1-Au-C4-C5). The potential energy curves along the dihedral angle $D_{C1\text{-}Au\text{-}C4\text{-}C5}$ from 0º to 90º (the energy at $D_{C1\text{-}Au\text{-}C4\text{-}C5}$ = 0º was used as the reference and each point relaxed).

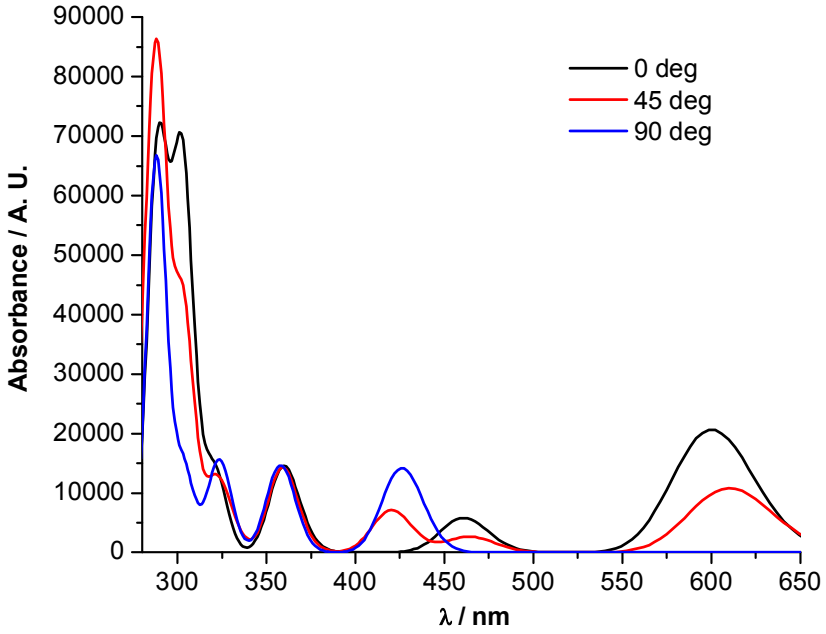


**Figure S7.** The simulated absorption spectra of complex **5** in acetonitrile based on three structures with dihedral angle (D) between the arylacetylide and the [Au(C^N^N)] plane of 0º, 45º and 90º, respectively.

**Discussion on Figure S6 and S7:**

To get insight into the effect of $NMe_2$ group on the absorption spectrum of **5**, a comparison of frontier molecular orbitals between that of **5** having a $C{\equiv}CC_6H_4$-$NMe_2$ ligand with that of **1** having a $C{\equiv}CC_6H_5$ ligand was performed (Figure 5). Although the orbital shapes are almost alike from HOMO-1 to LUMO for both **5** and **1**, the energy level of HOMO of **5** is lifted much higher, leading to a much smaller HOMO-LUMO gap (2.51 eV for **5** vs. 3.73 eV for **1**). This accounts for the different color of **5** and **1** in solid-state and in solutions. According to the geometrical optimization, the energetic minima were found with the dihedral angle (DA) between the arylacetylide and the [Au(C^N^N)] planes at 29.2º and 89.5º for **5** and **1**, respectively. This indicates that with the groups of $NMe_2$ and H at the *para*-position of the arylacetylide ligand, the cation structure of $[Au(C^N^N)(C{\equiv}CC_6H_4\text{-}4\text{-}R)]^+$ prefers coplanar and perpendicular configuration, respectively. However, potential energy curve scans along the DA shows that the total

energy differences between the coplanar and perpendicular configurations are very small (only about 0.5 and 0.3 kcal/mol for **1** and **5**, respectively). Such "barrier-less" rotation would be salient in both gas phase and in fluid solutions.

For the optimized structure (DA ≈ 90º) of **1**, the LLCT [π(arylacetylide)→π*(C^N^N)] transition(s) is symmetry forbidden, and the lowest allowed transition is LC [π→π*(C^N^N)] in nature, with absorption maximum at 359 nm, which well matches the experimental absorption peak maximum around 370 nm. The second lowest dipole allowed electron transition of **1** has mixed LMCT/LLCT characters [π(arylacetylide)→σ*[Au($d_{x2-y2}$)/(C^N^N)], and the calculated wavelength (324 nm) coincides with the experimental shoulder at around 325 nm. As for the optimized structure of **5** (Figure 6), the LC state has identical energy to that of **1**, being unaffected by the $NMe_2$ group, while the LMCT/LLCT state is significantly red-shifted to 418 nm because of the lifted HOMO with the effect of the $NMe_2$ group. Notably, with DA deviated from 90º, the LLCT states of **5** are "switched-on", although their energies (463 nm and 605 nm) were underestimated when compared with that of the experimental values (an absorption tail in the 450−525 nm range). This less satisfactory agreement between the calculated and the experimental absorption energies of the LLCT state is not unexpected as using TDDFT to accurately calculate the energy of such a long-range charge transfer state still remains a challenge.[i] Notably, for **5** with the "barrier-less" rotation, the LMCT/LLCT states can be "switched-off" around the coplanar configuration and the LLCT state "switched-on" around the perpendicular configuration.

In summary, the $NMe_2$ group of the arylacetylide ligand not only renders the molecule towards a coplanar configuration, switching on the LLCT state, but also significantly lowers the energy of the LLCT state through lifting the HOMO, leading to the LLCT state energetically distinguished from other excited states (including LMCT and ILCT). This implies that new specific and distinct spectral properties could be anticipated if the barrier of the rotation of the arylacetylide ligand is increased by chemical modifications (such as bulky substitutes) or by physical methods (such as change in the solvent viscosity).

**Table S3.** The energy ($E_{ex}$ in eV, followed by wavelength in nm in parenthesis) and oscillator strength (*f* in a.u.) of each excited state calculated by PBE0 with solvation of acetonitrile.

| | | Complex **5** | | | Complex **1** | | |
|---|---|---|---|---|---|---|---|
| $D_{C1\text{-}Au\text{-}C4\text{-}C5}$ | | 0º | 45º | 90º | 0º | 45º | 90º |
| $S_1$ | $E_{ex}$ | 2.07 (600) | 2.03 (610) | 2.00 (619) | 3.15 (394) | 3.11 (399) | 3.07 (403) |
| | *f* | 0.142 | 0.074 | 0.000 | 0.124 | 0.059 | 0.000 |
| $S_2$ | $E_{ex}$ | 2.69 (461) | 2.67 (464) | 2.65 (467) | 3.45 (360) | 3.45 (360) | 3.45 (359) |
| | *f* | 0.040 | 0.018 | 0.000 | 0.095 | 0.095 | 0.096 |
| $S_3$ | $E_{ex}$ | 2.98 (416) | 2.95 (420) | 2.91 (426) | 3.80 (326) | 3.78 (328) | 3.76 (330) |
| | *f* | 0.001 | 0.049 | 0.098 | 0.051 | 0.021 | 0.000 |
| $S_4$ | $E_{ex}$ | 3.35 (370) | 3.33 (372) | 3.32 (374) | 3.85 (322) | 3.84 (323) | 3.83 (324) |
| | *f* | 0.008 | 0.004 | 0.000 | 0.000 | 0.028 | 0.058 |
| $S_5$ | $E_{ex}$ | 3.45 (359) | 3.45 (359) | 3.46 (358) | 3.86 (321) | 3.90 (318) | 3.94 (315) |
| | *f* | 0.097 | 0.098 | 0.101 | 0.001 | 0.055 | 0.092 |
| $S_6$ | $E_{ex}$ | 3.72 (334) | 3.76 (330) | 3.83 (323) | 4.05 (306) | 4.08 (304) | 4.11 (302) |
| | *f* | 0.000 | 0.023 | 0.107[a] | 0.113 | 0.097 | 0.078 |
| $S_7$ | $E_{ex}$ | 3.87 (320) | 3.86 (321) | 3.83 (324) | 4.12 (301) | 4.12 (301) | 4.13 (301) |
| | *f* | 0.098 | 0.077 | 0.000[a] | 0.001 | 0.001 | 0.001 |
| $S_8$ | $E_{ex}$ | 4.04 (307) | 4.04 (307) | 4.04 (306) | 4.29 (289) | 4.28 (289) | 4.27 (290) |
| | *f* | 0.001 | 0.000 | 0.000 | 0.000 | 0.007 | 0.000 |
| $S_9$ | $E_{ex}$ | 4.07 (305) | 4.08 (304) | 4.09 (303) | 4.30 (288) | 4.31 (288) | 4.32 (287) |
| | *f* | 0.078 | 0.083 | 0.099 | 0.221 | 0.254 | 0.337 |
| $S_{10}$ | $E_{ex}$ | 4.10 (303) | 4.09 (303) | 4.10 (302) | 4.45 (279) | 4.43 (280) | 4.40 (281) |
| | *f* | 0.374 | 0.0202 | 0.000 | 0.008 | 0.005 | 0.000 |

[a]: For the conformer with $D_{C1\text{-}Au\text{-}C4\text{-}C5}$ = 90º, the energy $S_6$ is very slightly smaller than $S_7$, but in order to compare the states with same characters, $S_6$ and $S_7$ were exchanged artificially.

**Discussion on Table S3:**

Considering the "barrier-less" rotation of the ligand C≡C$C_6H_5$-4-$NMe_2$, besides the excited states of optimized structure, the excited states of more three structures (with $D_{C1\text{-}Au\text{-}C4\text{-}C5}$ fixed at 0º, 45º and 90º) were calculated. Both the coplanar conformer ($D_{C1\text{-}Au\text{-}C4\text{-}C5}$ = 0º) and the perpendicular conformer ($D_{C1\text{-}Au\text{-}C4\text{-}C5}$ = 90º) are close to $C_s$ symmetry, which involve two types of characters (A′ and A″) of molecular orbitals. In coplanar conformer, HOMO, involving $\pi_{[C\equiv CPhN(CH3)2]}$, belongs to A″, which can be excited to LUMO (A″), while in perpendicular conformer, HOMO belongs to A′, which can't be excited to LUMO (A″), in such a linear alignment along ligand-Au-ligand′. Thus,

all pure LLCT states tabled in Table S3 are switched off from the coplanar conformer to perpendicular one, while a LMCT state ($S_3$, $\pi_{[C\equiv CC6H5\text{-}4\text{-}NMe2]}\rightarrow\sigma^*_{[Au(dx2\text{-}y2)\sim(C\text{^}N\text{^}N)]}$) is switched on in the perpendicular conformer, because it is a $A''\rightarrow A'$ transition in the coplanar conformer. Only LC ($\pi\rightarrow\pi^*_{[C\text{^}N\text{^}N]}$) states $S_5$ and $S_9$ are always active.

For **1**, similar switch effects of the spectra were seen. Since the group $-N(CH_3)_2$ has not effects on the energies of HOMO-1 and LUMO orbitals of **5** relative to **1** (see Figure S7 ), their HOMO-1→LUMO ILCT ($\pi\rightarrow\pi^*_{[C\text{^}N\text{^}N]}$) states, $S_5$ (359 nm) of **5** and $S_2$ (359 nm) of **1** (Table 1), have identical values of energy. However, because of more deeply occupied HOMO in **1**, the state $S_4$ (Table S3) with LMCT character has a wavelength of 324 nm, corresponding to $S_3$ (Table S3) in **5**, with a wavelength of 418 nm.

The Cartesian coordinate of the optimized structure and the lowest 3 frequencies for **1**:

H,3.1443263479,4.531080701,18.9162513313
C,3.0818032003,4.1014184853,19.9067160241
C,1.8806771325,3.5741341797,20.3745687204
C,4.1930031799,4.0663773986,20.7297398562
C,0.5881511565,3.4972387826,19.6998212503
Au,0.1061374176,2.3105831417,22.2293479974
N,1.8647519002,3.0546872997,21.6116592334
H,5.1322665221,4.4739936964,20.3751930752
C,4.1279848282,3.5167360631,22.0067093806
N,1.3698202858,1.9482607643,23.9398485851
C,2.9176666152,3.0028530745,22.4362598031
C,-1.6014795659,1.5886100139,22.8277020337
H,5.0042495424,3.4958697736,22.6394480655
C,2.6373979692,2.3795379022,23.7470158854
C,1.0165698903,1.3739531119,25.0842988934
C,-2.648308838,1.130029187,23.2329203379
C,3.5865816897,2.227754365,24.7428920904
C,1.9214825468,1.1945772303,26.1169941461
H,-0.018316469,1.0576649957,25.1556517009
C,-0.4840228819,2.9050260999,20.4092812427
C,0.3647032457,3.9721905632,18.4105504616
C,-3.8770332007,0.5909049939,23.7105278332
H,4.6005789892,2.5720851035,24.5902726093
C,3.223060011,1.6287217486,25.9399277212
H,1.6012964289,0.722971296,27.0367661415
C,-1.7321628564,2.7979233487,19.8366655221
C,-4.7854030858,1.40247576,24.3973548893
C,-4.1900675331,-0.7546813353,23.4939286715
C,-0.8911220515,3.8632651969,17.8371870998
H,1.1712174486,4.4294280253,17.8486327818
H,-2.5464277841,2.3440392535,20.3854023497
C,-1.9309265154,3.2806745417,18.545077453
H,-4.5457486557,2.445871146,24.563617553
C,-5.9797909689,0.8751003012,24.8557816602
C,-5.3869936632,-1.272856948,23.956210022
H,-3.4886953362,-1.3842245379,22.9596040143
H,3.9566967475,1.5040554862,26.7273193865
H,-1.0581967968,4.2348220995,16.8337267812
H,-2.9125587984,3.1970172054,18.0933485574
H,-6.6787897166,1.5114525417,25.3857535432
C,-6.2837325492,-0.461462331,24.6373709253
H,-5.6223750601,-2.3163583801,23.7826754965
H,-7.220477769,-0.8706193455,24.9970408731

Harmonic frequencies (cm**-1), IR intensities (KM/Mole), Raman scattering activities (A**4/AMU), depolarization ratios for plane and unpolarized incident light, reduced masses (AMU), force constants (mDyne/A), and normal coordinates:

| | 1 | 2 | 3 |
|---|---|---|---|
| | A | A | A |
| Frequencies -- | 11.9482 | 19.3731 | 20.6121 |
| Red. masses -- | 3.7184 | 6.4376 | 5.9582 |
| Frc consts -- | 0.0003 | 0.0014 | 0.0015 |
| IR Inten -- | 0.0131 | 0.3843 | 1.1341 |

The Cartesian coordinate of the optimized structure and the lowest 3 frequencies for **5**

H,3.1112544592,4.5173380187,18.8977994127
C,3.0539672112,4.1018525249,19.894642993
C,1.862803074,3.5559550739,20.3651126447
C,4.1620254471,4.1067672385,20.7234189004
C,0.5741763867,3.4458192258,19.6886178878
Au,0.1056809788,2.2907519456,22.2356692435
N,1.8512825565,3.0542217785,21.6105114328
H,5.093204198,4.5307455058,20.3669675888
C,4.1020416406,3.5774608402,22.0088210578
N,1.3692817524,1.980414626,23.9529716423
C,2.9019216772,3.0414264202,22.4406666901
C,-1.5842373508,1.5450161057,22.8379517375
H,4.9745143229,3.5885054008,22.6470949828
C,2.6308079294,2.428547506,23.7564089294
C,1.0268648291,1.4043999729,25.1002396374
C,-2.6340983159,1.1009523218,23.2612131932
C,3.5829797187,2.2959997025,24.7532270844
C,1.9340309875,1.2458523545,26.1333781491
H,-0.0017977565,1.068364871,25.1703209931
C,-0.4909445526,2.8531551678,20.4086291517
C,0.3461182894,3.8966398809,18.391004012
C,-3.8558800749,0.5706751767,23.7394667678
H,4.5922220931,2.652258472,24.5965093826
C,3.2293004094,1.6995618602,25.9535029496
H,1.6221267288,0.7738871824,27.0557579874
C,-1.7384323588,2.726599096,19.8369389008
C,-4.1772367122,0.5887307879,25.1023584708
C,-4.7925584962,0.0095623975,22.8618313639
C,-0.9076913808,3.7651351008,17.8194072158
H,1.148136828,4.353373376,17.8222536653
H,-2.548135022,2.2777583784,20.3962840994
C,-1.9422138882,3.185234208,18.5382765199
H,-3.4759770041,1.0228901634,25.8057325966

C,-5.3665586436,0.0785965145,25.5690268
C,-5.9839864994,-0.5071175943,23.3150306137
H,-4.5699913806,-0.023408859,21.8016299892
H,3.9652070505,1.5899124567,26.7409790418
H,-1.0784910923,4.1179098215,16.8097920307
H,-2.9232954632,3.0860904167,18.0883754438
H,-5.5703292754,0.120619173,26.6299169529
C,-6.3104983519,-0.4881425065,24.6871989697
H,-6.6726925627,-0.9318898383,22.5980777789
N,-7.4876394954,-0.99560371,25.1411599162
C,-8.4348561647,-1.568755467,24.2169249788
C,-7.7999181526,-0.9569070018,26.5483219848
H,-8.0095427285,-2.4209645417,23.6752231825
H,-8.781608002,-0.8347617334,23.4806973506
H,-9.302276784,-1.9236535996,24.7688186841
H,-7.0736775345,-1.5228909563,27.1426880734
H,-8.7800708141,-1.4001474238,26.7089820731
H,-7.8285157105,0.0695761683,26.9309548511

Harmonic frequencies (cm**-1), IR intensities (KM/Mole), Raman scattering activities (A**4/AMU), depolarization ratios for plane and unpolarized incident light, reduced masses (AMU), force constants (mDyne/A), and normal coordinates:

| | 1 | 2 | 3 |
|---|---|---|---|
| | A | A | A |
| Frequencies -- | 9.4261 | 14.5741 | 16.7694 |
| Red. masses -- | 3.2424 | 5.6893 | 5.7929 |
| Frc consts -- | 0.0002 | 0.0007 | 0.0010 |
| IR Inten -- | 0.3020 | 0.7432 | 2.4374 |

[i] a) A. Dreuw, M. Head-Gordon, *J. Am. Chem. Soc.* **2004**, *126*, 4007–4016; b) G. L. Cui, W. T. Yang, *Mol. Phys.* **2010**, *108*, 2745–2750.